Studies of Co·Bleomycin A2 Green: Its Detailed Structural Characterization by NMR and Molecular Modeling and Its Sequence-Specific Interaction with DNA Oligonucleotides

Wei Wu,[†,⊥] Dana E. Vanderwall,[‡,⊥] Siu Man Lui,[†] Xue-Jun Tang,[||] Christopher J. Turner,*[,§] John W. Kozarich,*[,‡,▽] and JoAnne Stubbe*[,†]

Contribution from the Departments of Chemistry and Biology, Massachusetts Institute of Technology, Cambridge, Massachusetts 02139, Department of Chemistry and Biochemistry, University of Maryland, College Park, Maryland 20742, Francis Bitter Magnet Laboratory, Massachusetts Institute of Technology, Cambridge, Massachusetts 02139, and Department of Biochemistry, Albert Einstein College of Medicine, Bronx, New York 10461

Received July 25, 1995[⊗]

Abstract: The structure of homogeneous Co·Bleomycin (CoBLM) A2 green (the hydroperoxide form of CoBLM) has been determined using 2D NMR methods and molecular dynamics calculations. Previous studies of Xu et al. (Xu, R. X.; Nettesheim, D.; Otvos, J. D.; Petering, D. H. *Biochemistry* **1994**, *33*, 907−916) reported several possible structures for CoBLM A2 green compatible with their NMR data acquired on a mixture of CoBLM A2 green and A2 brown forms. The availability of the pure CoBLM A2 green, which is stable for months at neutral pH, has allowed the complete assignments of the ^{1}H and ^{13}C chemical shifts, observation of 55 intramolecular NOEs, and determination of 15 coupling constants allowing the definition of dihedral angles. These results are a prerequisite to determining its structure with duplex DNA of a defined sequence (Wu, W.; Vanderwall, D. E.; Turner, C. J.; Kozarich, J. W.; Stubbe, J. *J. Am. Chem. Soc.* **1996**, *118*, 1281−1294). Two screw sense isomers each containing two possible axial ligands (the primary amine of the β-aminoalanine and the carbamoyl nitrogen of the mannose) were considered as viable candidates for the structure of CoBLM A2 green. Using the NMR constraints and molecular dynamics calculations, the structures of all four isomers were generated. One set of screw sense isomers can be readily eliminated from considerations based on violations of NOE and dihedral angle constraints. The other screw sense isomer containing either one or the other of the postulated axial ligands has been examined in some detail. The structure containing the primary amine of β-aminoalanine as the axial ligand is favored on the basis of coupling constants and NOE arguments, potential energy considerations, model studies, and studies with analogs of BLM. The favored structure is compact with the bithiazole moiety folded back underneath the equatorial plane of the metal binding domain, on the same face as the hydroperoxide ligand. The geometry of the peptide linker is very well defined by the observed coupling constants in the valeryl and threonine moieties of the linker. CoBLM A2 green has been studied with two self-complementary oligonucleotides, d(CCAGGCCTGG) and d(CCAGTACTGG). Both of these oligomers possess a single, UV light-mediated cleavage site (C and T, respectively). In addition, fluorescent quenching studies have allowed the determination of the first sequence-specific dissociation constants of 1.7×10^{-7} and 1.5×10^{-7} M, respectively. Titration of CoBLM A2 green with each of these oligomers reveals a 1:1 complex in slow exchange on the NMR time scale. The upfield shifts of the bithiazole protons in both of these complexes are indicative of a partial intercalative mode of binding. The stage is now set for the determination of the structure of the CoBLM A2 green bound sequence specifically to DNA.

Introduction

Since the discovery of bleomycins (BLMs) by Umezawa and co-workers and their recognition as antitumor agents,[1] much effort has been focused on understanding the basis for their therapeutic efficacy and their side effects.[2] Seminal experiments by Peisach and Horwitz and their co-workers[3] revealed that two cofactors, a metal and O_2, are required for the BLMs to degrade double-stranded (ds) DNA, the presumed therapeutic target. Recent studies have also shown that unusual tertiary structures of RNA as well as RNA/DNA hybrids are susceptible to degradation by metallo-BLMs.[4] While the mechanisms of degradation of DNA by the BLMs are understood at a moderately detailed molecular level,[5,6] the structural basis for the molecular recognition responsible for the observed sequence specificity of this cleavage has yet to achieve a comparable level of resolution.

The observation that BLM cleaves DNA by specific 4′-hydrogen atom abstraction supports the hypothesis that the metal binding domain (Figure 1) interacts specifically within the minor

[†] Departments of Chemistry and Biology, Massachusetts Institute of Technology.
[‡] University of Maryland.
[§] Francis Bitter Magnet Laboratory, Massachusetts Institute of Technology.
[||] Albert Einstein College of Medicine.
[⊥] Both authors contributed equally to this work.
[▽] Present Address: Merck Research Laboratories, P.O. Box 2000, Rahway, NJ 07065-0900.
* Authors to whom correspondence should be addressed.
[⊗] Abstract published in *Advance ACS Abstracts,* January 15, 1996.

(1) Umezawa, H.; Maeda, K.; Takeuchi, T.; Okami, Y. *J. Antibiot.* **1966**, *19,* 200−209.
(2) (a) Sikic, B. I.; Rozencweig, M.; Carter, S. K. Eds., In *Bleomycin Chemotherapy*; Academic Press: Orlando, FL, 1985. (b) Umezawa, H. In *Anticancer agents based on natural product models*; Cassady, J. M., Douros, J., Eds.; Academic Press, Inc.: New York, 1980; Vol. 16, pp 147−166. (c) Hecht, S. M. Ed. In *Bleomycin: Chemical, Biochemical, and Biological Aspects*; Springer-Verlag: New York, 1979.
(3) (a) Sausville, E. A.; Peisach, J.; Horwitz, S. B. *Biochem. Biophys. Res. Commun.* **1976**, *73*, 814−822. (b) Sausville, E. A.; Peisach, J.; Horwitz, S. B. *Biochemistry* **1978**, *17,* 2740−2746.

0002-7863/96/1518-1268$12.00/0

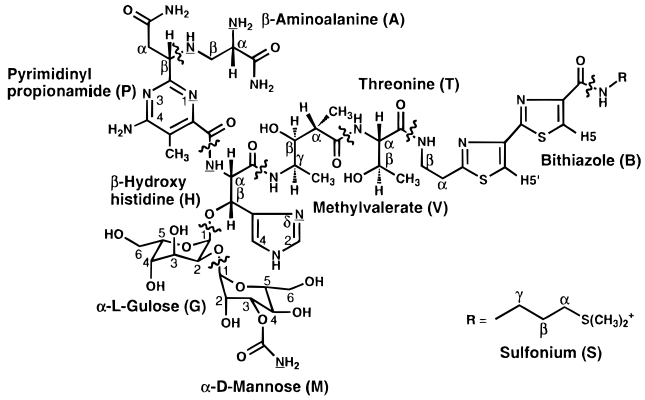

Figure 1. Structure of bleomycin A2.

groove.[7] This model is further corroborated by the observations that reagents known to specifically block, covalently or noncovalently, the minor groove, such as anthramycin and distamycin, inhibit BLM-mediated DNA degradation.[8,9] Furthermore, studies of Kuwahara and Sugiura using homopolymers of poly(dG)·poly(dC) and poly(dI)·poly(dC) show significantly reduced binding in the latter case, supporting the importance of the 2-amino group of guanine in the minor groove in a position 5′ to the cleavage site.[9] Recent cleavage studies using sequence specific incorporation of deoxyinosine into defined fragments of DNA also substantiate these earlier studies on homopolymers.[10]

On the other hand, major groove modifiers aflatoxin B (a guanine N-7 binder), 5-methylcytidines, and 5-(glucosyloxy)-methyl groups all seem to have little effect on the ability of BLM to mediate DNA degradation.[11−13] However, the methylation of the N-6 moiety of adenosine, also in the major groove, does perturb DNA cleavage.[13] The reasons for this are at present not known, and the results contradict other studies with major groove binders.

Over the past decade, a variety of biophysical methods have been used to define the role of the bithiazole moiety of BLM in binding to DNA. Early studies of Porvirk et al.[14] monitoring the unwinding and lengthening of DNA upon binding of BLM provided the first experimental evidence for intercalation of the bithiazole rings (Figure 1). Results of other methods including NMR studies with poly(dA-dT), viscometric studies, and fluorescence quenching studies as a function of ionic strength have been interpreted to support multiple modes of binding, including one involving partial intercalation of the bithiazole rings.[15] Very recent studies of Wu et al. on CoBLM A2 green binding to a d(CCAGGCCTGG), where C is the site of cleavage, have established unambiguously that the mode of binding is specific and involves partial intercalation.[16] Alternatively, recent studies of Manderville et al.[17] with ZnBLM and a defined oligomer have indicated multiple modes of binding, including one involving binding of the bithiazole tail within the minor groove as originally proposed by Dickerson.[18] Thus, there is no consensus regarding the binding mode(s), although the bithiazole moiety clearly provides binding energy. That different metallo-BLMs in different sequence contexts have alternative binding modes cannot be excluded.

Recent studies from the Hecht laboratory using synthetic BLM congeners suggest that the sequence selectivity of cleavage is governed almost completely by the metal binding domain of BLM.[5] This hypothesis is supported by their studies using a series of demethylated BLM and deglyclo-BLM A2 analogs in which the bithiazole C-terminus was separated from the metal binding domain by replacing the threonine moiety (Figure 1) with oligomeric glycine spacers of different lengths ($n = 0$, 1, 2, or 4).[19] The specificity of the cleavage pattern with these analogs ($n = 1$, 2, or 4) was very similar to the corresponding demethylated, deglyco-BLM A2 itself, thus supporting the hypothesis that specificity is governed by the metal binding domain. This proposal is further supported by studies with phleomycin (PLE), a BLM analog in which the bithiazole moiety is replaced by a thiazolinylthiazole, that is, the penultimate thiazolium ring is reduced and nonplanar (Figure 1). The sequence specificity of PLE, despite this altered structure, is almost identical to the that of BLM.[20] This observation has dampened the enthusiasm for the partial intercalative mode of binding of the bithiazole tail and has been interpreted as strong support for the importance of the metal binding domain in specificity.

Perhaps the most dramatic evidence defining the importance of the metal binding domain in specificity is the remarkable claim of Mascharak and co-workers that a synthetic BLM analog (Fe^{2+}(PMA)Cl·MeOH) lacking the sugars, peptidyl linker, and bithiazole tail, also exhibits the same sequence selectivity as BLM, although cleavage requires much higher concentrations.[21] Studies of the Boger laboratory,[22b] however, in which the metal binding domain (without the sugars) of BLM was assayed for cleavage specificity, revealed no cleavage. In addition, their studies with the metal binding domain containing the two sugars gave nonspecific cleavage.[22a] Furthermore, studies by Hecht

(4) (a) Hecht, S. M. *Bioconjugate Chem.* **1994**, *5*, 513−526. (b) Absalon, M. J.; Krishnamoorthy, C. R.; McGall, G.; Kozarich, J. W.; Stubbe, J. *Nucleic Acids Res.* **1992**, *20*, 4179−4185. (c) Krishnamoorthy, C. R.; Vanderwall, D. E.; Kozarich, J.; Stubbe, J. *J. Am. Chem. Soc.* **1988**, *110*, 2008−2009. (d) Morgan, M.; Hecht, S. M. *Biochemistry* **1994**, *33*, 10286−10293. (e) Holmes, C. E.; Carter, B. J.; Hecht, S. M. *Biochemistry* **1993**, *32*, 4293−4307. (f) Magliozzo, R. S.; Peisach, J.; Ciriolo, M. R. *Mol. Pharmacol.* **1989**, *35*, 428−432.

(5) Kane, S. A.; Hecht, S. M. in *Progress in Nucleic Acid Research and Molecular Biology*; Cohn, W. E., Moldave, K., Eds.; Academic Press: San Diego, CA, 1994; Vol. 49, pp 313−352.

(6) Stubbe, J.; Kozarich, J. W. *Chem. Rev.* **1987**, *87*, 1107−1136.

(7) Wu, J. C.; Stubbe, J.; Kozarich, J. W. *Biochemistry* **1985**, *24*, 7569−7573.

(8) Sugiura, Y.; Suzuki, T. *J. Biol. Chem.* **1982**, *257*, 10544−10546.

(9) Kuwahara, J.; Sugiura, Y. *Proc. Natl. Acad. Sci. U.S.A.* **1988**, *85*, 2459−2463.

(10) Zhang, G. Ph.D. Thesis, University of Maryland, 1993.

(11) Suzuki, T.; Kuwahara, J.; Sugiura, Y. *Biochem. Biophys. Res. Commun.* **1983**, *117*, 916−922.

(12) Long, E. C.; Hecht, S. M.; van der Marel, G. A.; van Boom, J. H. *J. Am. Chem. Soc.* **1990**, *112*, 5272−5276.

(13) Hertzberg, R. P.; Caranfa, M. J.; Hecht, S. M. *Biochemistry* **1988**, *27*, 3164−3174.

(14) Povirk, L. F.; Hogan, M.; Dattagupta, N. *Biochemistry* **1979**, *18*, 96−101.

(15) (a) Huang, C.; Galvan, L.; Crooke, S. T. *Biochemistry* **1980**, *19*, 1761−1767. (b) Chen, D. M.; Sakai, T. T.; Glickson, J. D.; Patel, D. J. *Biochem. Biophys. Res. Commun.* **1980**, *89*, 534−541.

(16) Wu, W.; Vanderwall, D. E.; Stubbe, J.; Kozarich, J. W.; Turner, C. J. *J. Am. Chem. Soc.* **1994**, *116*, 10843−10844.

(17) (a) Manderville, R. A.; Ellena, J. F.; Hecht, S. M. *J. Am. Chem. Soc.* **1994**, *116*, 10851−10852. (b) Manderville, R. A.; Ellena, J. F.; Hecht, S. M. *J. Am. Chem. Soc.* **1995**, *117*, 7891−7903.

(18) Dickerson, R. E. In *Mechanism of DNA Damage and Repair: Implications for Carcinogenesis and Risk Assessment Basic Life Sciences*; Smi, M. G., Grossman, L., Eds.; Plenum: New York, 1986; Vol. 38, pp 245−255.

(19) (a) Carter, B. J.; Murty, V. S.; Reddy, K. S.; Wang, S.-N.; Hecht, S. M. *J. Biol. Chem.* **1990**, *265*, 4193−4196. (b) Carter, B. J.; Reddy, K. S.; Hecht, S. M. *Tetrahedron* **1991**, *47*, 2463−2474.

(20) Kross, J.; Henner, W. D.; Hecht, S. M.; Haseltine, W. A. *Biochemistry* **1982**, *21*, 4310−4318.

(21) Guajardo, R. J.; Hudson, S. E.; Brown, S. J.; Mascharak, P. K. *J. Am. Chem. Soc.* **1993**, *115*, 7971−7977.

(22) (a) Boger, D. L.; Teramoto, S.; Honda, T.; Zhou, J. *J. Am. Chem. Soc.* **1995**, *117*, 7338−7343. (b) Boger, D. L.; Teramoto, S.; Zhou, J. *J. Am. Chem. Soc.* **1995**, *117*, 7344−7356.

and co-workers replacing each thiazolium ring with a methanethiol-like amino acid also showed nonspecific cleavage.[23]

It is clear from the above summary that the basis for molecular recognition is in strong need of structural information provided by either X-ray crystallographic or NMR spectroscopic methods. We have determined, using NMR methods, the structure of CoBLM A2 green and its binding to the self-complementary oligonucleotides d(CCAGGCCTGG) (**1**) and d(CCAGTACTGG) (**2**). This metallo-BLM was chosen as studies of Chang and Meares,[24] Saito et al.,[25] and McLean et al.,[26] and our own studies,[27] have revealed a sequence selectivity for cleavage similar to that observed with FeBLM. Three additional considerations led us to the choice of CoBLM A2 green: the ligands are exchange inert, the complex itself is diamagnetic, and the stable Co-hydroperoxide (CoOOH) is an excellent model of activated BLM (FeOOH). Furthermore, cleavage mediated by CoBLM A2 green occurs only in the presence of light and its binding affinity for generic DNA has been reported to be 10 times higher than that of the FeBLM.[24]

The utility of CoBLM A2 green as a model for activated BLM was also apparent to the Petering and Otvos laboratories.[28] In 1994, they reported chemical shift assignments of the mixture of CoBLM A2s (green and brown forms) using 2D NMR spectroscopic methods. Using their observed NOE constraints and molecular modeling, they described several structures of both the green (hydroperoxide as the sixth ligand) and brown (H_2O as the sixth ligand) forms of the CoBLMs which were consistent with their results. In both of the structures with CoBLM A2 green, their most interesting observation was that the bithiazole tail folded back, underneath, and across the metal binding domain. In one structure, the tail was on the same face as the putative hydroperoxide axial ligand (this is structure A in their nomenclature and will be defined as structure I subsequently). In the second structure, the tail was in a less energetically favorable conformation, on the opposite face from the hydroperoxide ligand (this is structure B in their nomenclature and will be defined here as structure III). At the time of their report, we had also completed a detailed 2D NMR study of CoBLM A2 green. In contrast to their report, in our hands, the green form is stable for several months at room temperature and at neutral pH and is easily isolable in excellent yields. We have, therefore, focused our efforts specifically on CoBLM A2 green.

This paper and its companion paper[48] report the details of 2D NMR studies which have been used to obtain a structural model providing, for the first time, the definition of the role of the bithiazole tail in binding to DNA and the basis for specificity of cleavage at d(G-Py). In this paper we report the detailed NMR studies of CoBLM A2 green which have allowed us to define unambiguously the screw sense of the ligand binding to the cobalt and the nature of the axial ligands.

The NMR assignment of the protons and carbons of CoBLM A2 green and the resulting structure by molecular modeling are just the first steps toward solving the structure of CoBLM A2 green with DNA. We also, therefore, report the studies of this CoBLM with two decameric self-complementary oligonucleotides, d(CCAGGCCTGG) and d(CCAGTACTGG), and show that cleavage occurs at a single pyrimidine (underlined) in each case. Fluorescent binding studies of CoBLM A2 green to the decamers have allowed us to determine the K_ds for a single binding site in each oligomer. Finally, preliminary NMR titration studies with d(CCAGTACTGG) are presented, which suggest that the mode of binding of CoBLM A2 green to this oligomer is similar to that reported for d(CCAGGCCTGG) in detail in the accompanying paper.

Materials and Methods

Preparation of CoBLM A2 Green. Blenoxane (15 units) provided by Bristol-Myers Co. was dissolved in H_2O and the pH adjusted to 7 with dilute NaOH. $CoCl_2$ (1.1 equiv) was then added to a rapidly stirred solution to ensure oxygenation, and the reaction was allowed to proceed for 2 h at room temperature. The mixture of products was separated using a semipreparative reverse-phase Alltech Econosil C-18 column (10 μm) and the elution system of 0.1 M ammonium acetate (pH 6.8) as solvent A and acetonitrile as solvent B. The products were eluted at a flow rate of 3 mL/min using a linear gradient from 12 to 15% A over 60 min (compound, retention time in min): CoBLM A2 brown, 13; CoBLM A2 green, 19; CoBLM B2 brown, 27; CoBLM B2 green, 40. The lyophilized samples were redissolved in 50 mM sodium phosphate, pH 6.8, and stored at −80 °C.

Extinction Coefficient of CoBLM A2 Green. The cobalt in the CoBLM A2 green was measured using a Varian AA-1475 atomic absorption spectrophotometer with a Varian GTA-95 graphite tube atomizer using a lamp current of 7 mA and a wavelength (λ) of 240.7 nm. CoBLM A2 green (50 μL of a 10 μM solution) was diluted with 1% (w/v) HNO_3 in a 5 mL volumetric flask and incubated for 12 h. A standard curve was prepared using a cobalt atomic absorption standard solution obtained from Aldrich which was diluted with 1% HNO_3 to 0.03−0.17 μM in cobalt. In the case of both the standards and the CoBLM A2 green, the protocol involves ashing at 900 °C for 40 s followed by atomization at 2300 °C for 4 s. The procedure was a modification of one previously reported for the quantitation of vitamin B_{12}.[29] The extinction coefficient was redetermined for vitamin B_{12} as a control. The extinction coefficient was $(2.1 \pm 0.2) \times 10^4$ M^{-1} cm^{-1} at 290 nm for CoBLM A2 green.

Characterization of CoBLM A2 Green by Electrospray Mass Spectrometry. All mass spectra were obtained using an PE-SCIEX API III triple-quadruple mass spectrometer (SCIEX, Thornhill, ON, Canada) equipped with an ionspray (pneumatically assisted electrospray) interface. A Macintosh computer was used for instrument control, data acquisition, and data processing. The CoBLM A2 green samples in deionized H_2O were introduced directly into the mass spectrometer at a flow rate of 2 μL/min using a syringe pump. Typically, mass scans were performed with a step size of 0.05−0.1 Da and a dwell time per step of 0.5−1 ms. Ten scans were usually accumulated to yield a mass spectrum. A mass spectrum with unit mass resolution (peak width of 1 Da) was first acquired for each sample to give a representative profile, then the resolution of the spectrometer was tuned to give a peak width of 0.3−0.5 Da (full width at half-maximum) across the mass range of interest, so that the doubly charged and triply charged species could be identified unambiguously.

Purification of d(CCAGGCCTGG) (1) and d(CCAGTACTGG) (2). Oligonucleotides **1** and **2** were synthesized on a 10 μmol scale at the MIT Biopolymer Laboratory. These oligomers with 5′-dimethoxytrityl (DMT) group retained were purified on a semipreparative reverse-phase C-18 HPLC column using a linear triethylammonium acetate (pH 7.0)/acetonitrile gradient (10% to 40% MeCN in 60 min). Under these conditions, the oligomers eluted at 50 min. The oligomer was then detritylated with 80% acetic acid for 1 h followed by extractions with ether. After lyophilization to dryness, each oligomer was exchanged into sodium phosphate buffer (pH 6.8) in a microdialysis chamber (Bethesda Research Laboratories) equipped with a Spectra/Por 6 (SPECTRUM) membrane (1000 MW cutoff). For the NMR experiments described subsequently, each oligonucleotide was lyophilized three times from 99.9% D_2O and finally dissolved in 99.996%

(23) Hamamichi, N.; Natrajan, A.; Hecht, S. M. *J. Am. Chem. Soc.* **1992**, *114*, 6278−6291.
(24) Chang, C.-H.; Meares, C. F. *Biochemistry* **1984**, *23*, 2268−2274.
(25) Saito, I.; Morii, T.; Sugiyama, H.; Matsura, T.; Meares, C. F.; Hecht, S. M. *J. Am. Chem. Soc.* **1989**, *111*, 2307−2308.
(26) McLean, M. J.; Dar, A.; Waring, M. J. *J. Mol. Recognit.* **1989**, *1*, 184−192.
(27) Worth, L., Jr.; Frank, B. L.; Christner, D. F.; Absalon, M. J.; Stubbe, J.; Kozarich, J. W. *Biochemistry* **1993**, *32*, 2601−2609.
(28) Xu, R. X.; Nettesheim, D.; Otvos, J. D.; Petering, D. H. *Biochemistry* **1994**, *33*, 907−916.
(29) Peck, E. *Anal. Lett.* **1978**, *B11*, 103−117.

D_2O. For experiments in H_2O, the lyophilized material was dissolved in 90% H_2O/10% D_2O. A typical DNA NMR sample contained 2 mM duplex in 50 mM sodium phosphate buffer (pH 6.8). Similar lyophilization procedures were carried out on CoBLM A2 green, and the final lyophilized product was redissolved in 99.996% D_2O at a final concentration of 2−5 mM.

Cleavage of 1 and 2 by CoBLM A2 Green. Oligomers **1** and **2** with the protecting groups removed were obtained from the MIT Biopolymer Laboratory. ^{32}P labeling of **1** and **2** on their 5′-ends was accomplished using T4 polynucleotide kinase and [γ-^{32}P]ATP purchased from New England Nuclear/Dupont. Labeled oligomer was separated from the unincorporated ^{32}P using a NENSORB-20 column (Dupont New England Nuclear).

Cleavage reactions were carried out in 80 μL containing 50 μM (in duplex) of unlabeled oligomer **1** (or **2**), and ∼5 μM [^{32}P]**1** (or **2**), 500 μM sodium phosphate buffer pH 7.0, and 50−200 μM CoBLM A2 green. Two control reactions (without UV light irradiation or without CoBLM) were also carried out. Each reaction mixture was transferred to a 6 × 50 mm Kimble borosilicate glass culture tube which was suspended from a copper wire in the center of a Rayonet photochemical reactor and irradiated at 350 nm for 10 min in a 4 °C cold room (the temperature in the center of the reactor was 20 °C). After the completion of irradiation, the DNA was isolated by making the solution 0.3 M in NaOAc and adding of 4 volumes of ethanol. The mixture was placed on dry ice for 20 min and the precipitated DNA isolated. The DNA pellets were then suspended in 100 μL of 10% piperidine at 90 °C for 10 min. The solution was cooled and subjected to a second ethanol precipitation. The recovered DNA pellets were suspended in the gel loading buffer (0.1% w/v bromophenol blue and 0.1% xylene cyanol) and loaded onto a 20% denaturing polyacrylamide sequencing gel (19:1 cross-link, 43 cm × 38 cm × 0.4 mm). The gel was run for 2 h at 90 W (constant power). The radioactivity was visualized using a Molecular Dynamics Phosphorimager with Image-Quant software (version 3).

Titration of CoBLM A2 Green with 1 and 2. The CoBLM A2 green concentration was determined optically ($\epsilon = 2.1 \times 10^4$ M^{-1} cm^{-1}) as described above. Absorbances of the duplexes **1** and **2** were measured at 260 nm, and their concentrations were determined from their calculated extinction coefficients $\epsilon = 1.0 \times 10^5$ M^{-1} cm^{-1} and $\epsilon = 1.2 \times 10^5$ M^{-1} cm^{-1}, respectively.[30] Various aliquots of CoBLM A2 green (0−1 equiv) were added to the solution of duplex in D_2O, and the complex formation was followed by monitoring the changes in the 1D ^{1}H NMR spectrum.

Determination of the Number of Binding Sites and K_ds of CoBLM A2 Green to 1 and 2 Monitoring the Fluorescence Changes. The binding parameters were obtained from the fluorescence measurements by methods analogous to those previously described by Chien et al.[31] and Chang and Meares.[24] Fluorescence intensities were measured at 353 nm on a Perkin-Elmer Fluorometer (LS 50) at 20 °C with excitation at 300 nm. Conditions were chosen so that each set of experiments covered as wide a range of percent-bound CoBLM as practical. A minimum of 1 μM CoBLM A2 green was needed for an adequate fluorescence intensity measurement. The K_d's are subject to some uncertainty since they were determined using μM solutions of CoBLM and are on the order of 10^{-7} M.

NMR Experiments. All 1D NMR spectra were recorded on a Varian VXR 500 MHz instrument or a home-built 500 MHz instrument in Francis Bitter Magnet Laboratory, and data were transferred to a Silicon Graphics XS24 workstation and processed using Felix software (version 2.3, Biosym Technologies, Inc.). ^{1}H and ^{13}C chemical shifts are referenced to an internal standard, sodium 3-(trimethylsilyl)-1-propanesulfonate (TSP), at 0.00 ppm.

2D NOESY (100, 200, and 400 ms mixing times), P. E. COSY, and TOCSY (MLEV-17 spin lock pulse with 35 and 70 ms mixing times) experiments on CoBLM A2 green in D_2O or 90% H_2O/10% D_2O were recorded at 5 °C. During the relaxation delay period the HDO solvent signal was selectively irradiated for 1.5 s. 2D NOESY experiments with a jump and return pulse sequence[32] were also collected at 100 and 200 ms mixing times. Data sets with 4096 complex points in t_2 and 512 complex points in t_1 were acquired with 5500 Hz sweep widths in both dimensions and 32 scans per t_1 increment. The t_1 dimension was zero-filled to 4096 data points. Spectra were processed with a combination of exponential and Gaussian weighting functions. Ridges in t_1 were reduced by multiplying the first point in t_1 by one-half prior to the Fourier transform. Baselines were corrected with a polynomial or an automatic baseline correction routine in t_2 when necessary.

^{1}H-Detected heteronuclear multiple-quantum coherence (HMQC)[33] (J_{C-H} set at 135, 165, or 195 Hz) and ^{1}H-detected heteronuclear multiple-bond correlation (HMBC)[34] (τ = 60 or 80 ms) experiments on CoBLM A2 green were recorded at 5 °C. During the relaxation delay period, the HDO solvent signal was selectively irradiated for 1.0 s. For the HMQC experiment, data sets with 2048 × 256 complex points were acquired with 6000 Hz sweep width in the proton dimension and 25 000 Hz in the carbon dimension. A total of 128 scans were collected per t_1 increment. For the HMBC experiments, data sets with 4096 × 256 complex points were acquired with the same sweep widths as in the HMQC experiments. A total of 64 scans were collected per t_1 increment. HMQC and HMBC spectra were processed with exponential weighting functions.

Molecular Modeling of CoBLM A2 Green. All calculations were carried out with Quanta 4.0/CHARMm 22 (Molecular Simulations Inc., Waltham, MA) on a Silicon Graphics 4D/35 or Indigo. Nonbonded van der Waals interaction was cutoff at 11.5 Å, using a cubic switching function between 9.5 and 10.5 Å. The distance-dependent dielectric constant algorithm in the CHARMm package was used. The nonbonded term was updated every 20 steps. The terms for electrostatic interactions and hydrogen bonds were not included in any calculations. The SHAKE algorithm[35] was used to fix all bond lengths to hydrogen atoms. Molecular dynamics calculations used the Verlet algorithm, with a 0.001 ps time step, and scaling every 100 steps. During molecular dynamics calculations, all force constants for bond distance and angles were set at 1000 kcal mol^{-1} Å^{-2} and 500 kcal mol^{-1} rad^{-2}, respectively. All energy minimizations used the standard CHARMm potential.[36] Distance constraints were applied using a square well potential and dihedral constraints were applied using a simple harmonic function.

Bleomycin A2 was constructed in Chemnote. Bond lengths between nitrogen and cobalt were set at 1.956 Å for the primary amine (axial ligand), 1.996 Å for the secondary amine, 1.851 Å for the N1 of pyrimidine, 1.910 Å for the histidine amide nitrogen, and 1.923 Å for the N_δ of the imidazole, based on the crystal structure of CoPMA-Cl.[37] The bond length for Co−O was set at 2.038 Å.[38] N−Co−N bond angles were set to 90°, and the axial N−Co−O (hydroperoxide) angle was set at 180°. Force constants of 288 kcal mol^{-1} Å^{-2} for Co−N bond lengths and 72 kcal mol^{-1} rad^{-2} for N−Co−N bond angles were derived from parameters used in the MM2 force field calculations on similar cobalt−N compounds.[39] A new CHARMm atom type was also created for a sulfonium sulfur atom. The parameters for bond lengths, bond angles, dihedral, and improper angles for the sulfur were determined by *ab initio* calculations using dimethylpropylsufonium cation as a model for the BLM sulfonium tail. Geometry optimization was carried out using the 3-21G* basis set and the Moller−Plesset correction (MP2) using Spartan (Wavefunction Inc., Irvine, CA). The

(30) (a) Cantor, C. R.; Warsaw, M. M. *Biopolymers* **1970**, *9*, 1059. (b) Puglisi, J. D.; Tinoco, I. J. *Methods Enzymol.* **1989**, *22*, 304−325.

(31) Chien, M.; Grollman, A. P.; Horwitz, S. B. *Biochemistry* **1977**, *16*, 3641−3647.

(32) Guéron, M.; Plateau, P.; Decorps, M. *Prog. Nucl. Magn. Reson. Spectrosc.* **1991**, *23*, 161.

(33) Bax, A.; Subramanian, S. *J. Magn. Reson.* **1986**, *67*, 565−569.

(34) Bax, A.; Summers, M. F. *J. Am. Chem. Soc.* **1986**, *108*, 2093−2094.

(35) van Gunsteren, W. F.; Berendsen, H. J. C. *Mol. Phys.* **1977**, *34*, 1311−1327.

(36) Brooks, B. R.; Bruccoleri, R. E.; Olafson, B. D.; States, D. J.; Swaminathan, S.; Karplus, M. *J. Comput. Chem.* **1983**, *4*, 187−217.

(37) Tan, J. D.; Hudson, S. E.; Brown, S. J.; Olmstead, M. M.; Mascharak, P. K. *J. Am. Chem. Soc.* **1992**, *114*, 3841−3853.

(38) Busch, D. H.; Jackson, P. J.; Kojima, M.; Chmielewski, P.; Matsumoto, N.; Stevens, J. C.; Wu, W.; Nosco, D.; Herron, N.; Ye, N.; Warburton, P. R.; Masarwa, M.; Stephenson, N. A.; Christoph, G.; Alcock, N. W. *Inorg. Chem.* **1994**, *33*, 910−923.

(39) (a) Hancock, R. D. *Prog. Inorg. Chem.* **1989**, *37*, 187−291. (b) Charles, R.; Ganly-Cunningham; Warren, R.; Zimmer, M. *J. Mol. Struct.* **1992**, *265*, 385−395.

charges for the CoBLM A2 green were determined using the template method of Quanta assuming a total charge of +2.0 and smoothing over all atoms. Color figures were made using Setor.[40]

Sizes of NOEs were classified as strong, medium, or weak on the basis of visual inspection of the NOESY spectra collected at 200 ms mixing time in D_2O and H_2O. NOE-derived distance constraints with a force of 60 kcal mol^{-1} Å^{-1} were set at 1.8−3.0, 1.8−4.0, and 1.8−5.0 Å for strong, medium, and weak NOEs, respectively. An additional 1 Å was added to the upper limit of the constraints on methyl or methylene hydrogen pseudoatoms. Coupling constants were measured in the 1D or 2D P.E. COSY spectra collected in D_2O and H_2O. A Karplus equation that considers the electronegativity of substituents[41] was used to derive dihedral angle constraints for the coupling constants not associated with the amide protons. Coupling constants involving amide protons were evaluated using the standard Karplus equation and the parameters of Hoch et al.[42] Because there is no evidence for any interaction between the sulfonium moiety of CoBLM A2 green and any other moiety within this molecule, dihedral constraints were used to maintain an extended conformation of this moiety.

Four models (vide infra), structures I, II, III, and IV of CoBLM A2 green (Figure 7), were used as starting structures for molecular dynamics simulated annealing calculations. The structures were first minimized with no constraints by the steepest descent method, followed by conjugate gradient minimization to a rms gradient of <0.1. The distance and dihedral constraints were then applied at 60 kcal mol^{-1} Å^{-2} and 50 kcal mol^{-1} rad^{-2}, and the minimization steps were repeated. These structures were used in the molecular dynamics simulated annealing calculations. For each structure five calculations were run starting with a different seed for the initial velocities. The structure was heated and equilibrated over 6 ps, from 5 to 1000 K in 10 K increments, with velocities assigned every 0.1 ps from a Gaussian approximation to the Maxwell−Boltzman distribution. No distance or dihedral angle constraints were used in this first step in order to randomize the structure prior to the application of the constraints. Molecular dynamics was then run for 4 ps with the distance constraints applied with a force constant of 0.06 kcal mol^{-1} Å^{-2}. Next, the force constants for the distance constraints were scaled to 120 kcal mol^{-1} Å^{-2} over 7.6 ps, in a series of 0.4 ps molecular dynamics runs. The system was allowed to evolve for 6 ps, then cooled to 300 K over 7 ps. At 300 K the force constants of the distance constraints were reduced to the final value of 60 kcal mol^{-1} Å^{-2}. The dihedral constraints were then introduced with a force constant of 50 kcal mol^{-1} rad^{-2}, and the system was allowed to equilibrate for 4 ps, followed by the final 15 ps molecular dynamics run. The coordinates of the final 5 ps of the 15 ps molecular dynamics were averaged and minimized by 1000 steps of conjugate gradient with distance and dihedral angle constraints.

Results and Discussion

Preparation and Characterization of CoBLM A2 Green. CoBLM A2 green has been prepared by a modification of the procedure of Chang et al.[43] from $CoCl_2$ and blenoxane. The reaction is complete within 2 h and the resulting products, hydroperoxide and aquo derivatives are separated using reverse-phase HPLC. CoBLM A2 green, the most efficient CoBLM mediator of DNA cleavage and a putative analog of activated BLM, was selected for examination in more detail. Given the time required for the acquisition of NMR data, the stability of this congener was examined by both HPLC and 1D NMR spectroscopy (data not shown). Both studies revealed that over a period of several months, at 20 °C and pH 7.0, that no change in the compound was detectable. These studies contrast with those reported by Xu et al.[44] for reasons that are at present not clear.

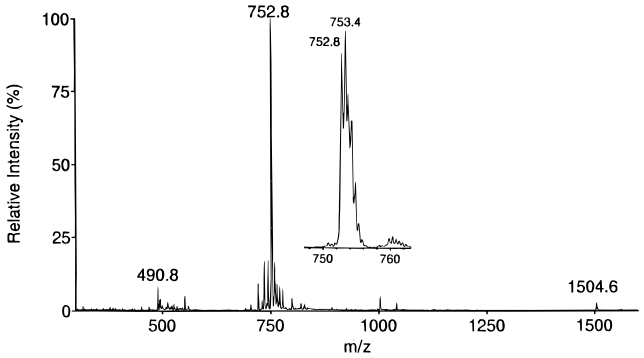

Figure 2. Electrospray mass spectrum of CoBLM A2 green. The inset shows the isotope distribution of the peak at *m*/*z* of 752.8.

Recent studies of Sam et al. investigating the structure of activated BLM (FeOOH) suggested that an excellent way to characterize a peroxide ligand, the putative sixth ligand in CoBLM A2 green, is by use of electrospray mass spectrometry.[45] This method is sufficiently mild that the OOH ligand is not lost during the analysis. An electrospray mass spectrum of CoBLM A2 green is shown in Figure 2. It gives a *m*/*z* of 752.8 (calculated MW = 1505.4, *m*/*z* = 752.7), which indicates that the charge of this form of CoBLM is +2. This result suggests, given the assumption that the charge of CoBLM in solution is similar to that observed by mass spectrometry, that the histidine amide must be deprotonated and is consistent with the sixth ligand being $^-$OOH. However, the spectrum shows that the isotopic distribution differs from that calculated[46] (see inset in Figure 2). Why this species has a mass at 753.4, significantly larger than the expected 72% contribution calculated from isotopic distributions, is at present not clear. Despite this anomaly, these studies provide strong support for the proposal of Chang and Meares[43] that CoBLM A2 green contains a hydroperoxide ligand. The stability studies in conjunction with the mass spectrometric characterization thus suggest that CoBLM A2 green is an appropriate choice for characterization by NMR spectroscopic methods.

Choice of Oligonucleotides and Their Interactions with CoBLM A2 Green. Several considerations led to the choice of oligomers to be used in NMR structural investigations. Self-complementary decameric oligonucleotides were chosen as the resulting duplexes and were sufficiently stable to allow data acquisition at 20 °C. The sequences were also chosen to contain a single CoBLM binding site and a single cleavage site. In addition, the self-complementarity facilitates the assignments of the proton chemical shifts and the determination of whether a single CoBLM binding site was present during a titration with CoBLM monitored by 1D NMR spectroscopy.

Two oligomers, d(CCAGGCCTGG) (**1**) and d(CCAG-TACTGG) (**2**), fulfilled these requirements. In both cases, when 5′-^{32}P-end labeled oligomer was incubated with CoBLM A2 green and subjected to light-mediated cleavage, a single major cleavage product subsequent to the piperidine treatment[27] was observed (Figure 3, cleavage shown for d(CCAGGCCTGG)). This major product persists even when the ratio of drug to oligomer is 4:1. These results and the fact that structural

(40) Evans, S. V. *J. Mol. Graphics* **1993**, *11*, 134−138.
(41) Haasnoot, C. A. G.; De Leeuw, F. A. A. M.; Altona, C. *Tetrahedron* **1980**, *36*, 2783−2792.
(42) Hoch, J. C.; Dobson, C. M.; Karplus, M. *Biochemistry* **1985**, *24*, 3831−3841.
(43) Chang, C.-H.; Dallas, J. L.; Meares, C. F. *Biochem. Biophys. Res. Commn.* **1983**, *110*, 959−966.
(44) Xu, R. X.; Antholine, W. E.; Petering, D. H. *J. Biol. Chem.* **1992**, *267*, 944−949.
(45) Sam, J. W.; Tang, X.-J.; Peisach, J. *J. Am. Chem. Soc.* **1994**, *116*, 5250−5256.
(46) Theoretical isotopic distribution for CoBLM A2 green is as follows: 752.7, 100%; 753.2, 72%; 753.7, 44%; 754.2, 19%.

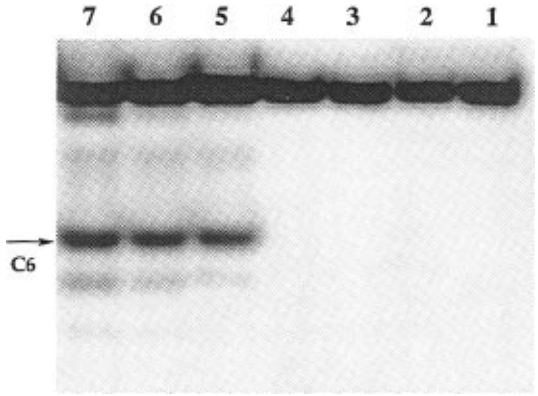

Figure 3. Autoradiography of a 20% denaturing polyacrylamide gel showing single-site cleavage by CoBLM A2 green on the 5′-^{32}P-labeled d(CCAGGCCTGG) (**1**) (lanes 1−4 are controls): lane 1, DNA without CoBLM but with UV light and with piperidine treatment; lane 2, DNA with CoBLM but with no light and with piperidine treatment; lane 3, same as lane 1 but with no piperidine treatment; lane 4, same as Lane 2 but with no piperidine treatment; lanes 5−7, reactions with different ratios of CoBLM A2 green to DNA with UV light and piperidine treatment; lane 5, 1:1 CoBLM A2 green:DNA; lane 6, 2:1 CoBLM A2 green:DNA; lane 7, 4:1 CoBLM A2 green:DNA.

information was available on the duplex DNA alone,[47] solidified our choice of d(CCAGGCCTGG) for further investigation as described in the companion paper.[48]

In an effort to determine whether a single cleavage site is correlated with a single binding site, each oligomer was titrated with CoBLM A2 green and changes in fluorescence were monitored. Previous studies revealed that binding of FeBLM and CoBLM to generic DNA resulted in fluorescence quenching.[24,31] A Scatchard analysis of the data (not shown) confirmed that both **1** and **2** appear to have a single CoBLM binding site with apparent K_ds on the order of 1.7×10^{-7} M and 1.5×10^{-7} M for d(CCAGGCCTGG) and d(CCAGTACTGG), respectively. These values are similar to the one previously reported by Chang and Meares of $\sim 10^{-7}$ M for generic calf thymus DNA at pH 8.0.[24]

Titration of CoBLM A2 Green with d(CCAGTACTGG) (2). Recent studies of Absalon et al. have revealed that GTAC is a "hot spot" for double-stranded cleavage (at T) with the ratio of ss:ds cleavage being 3:1.[49] In order to determine whether the mode of binding at GT steps is the same as GC steps and to establish whether binding of CoBLM A2 green can be detected at both the primary and the secondary cleavage sites involved in ds cleavage, preliminary studies with **2** were carried out. A typical titration of CoBLM A2 green with **2**, analyzed by 1D NMR spectroscopy, is shown in Figure 4 (6.5−9.5 ppm). Several features suggest that the predominant species is a ∼1:1 complex between CoBLM A2 green and **2**. The major complex is in slow exchange on the NMR time scale. In the free DNA (Figure 4a), two resonances at 8.24 and 8.26 ppm have been assigned to the H8 protons of A3 and A6, respectively. Upon addition of 0.5 equiv of CoBLM A2 green (Figure 4b), these resonances diminish in intensity and four new resonances appear. Upon addition of 1 equiv of CoBLM A2 green, the A-H8 protons of the free DNA have disappeared and the same four resonances have increased in intensity. Similarly, in the upfield region of the NMR spectrum, between 0 and 3.5 ppm (data not

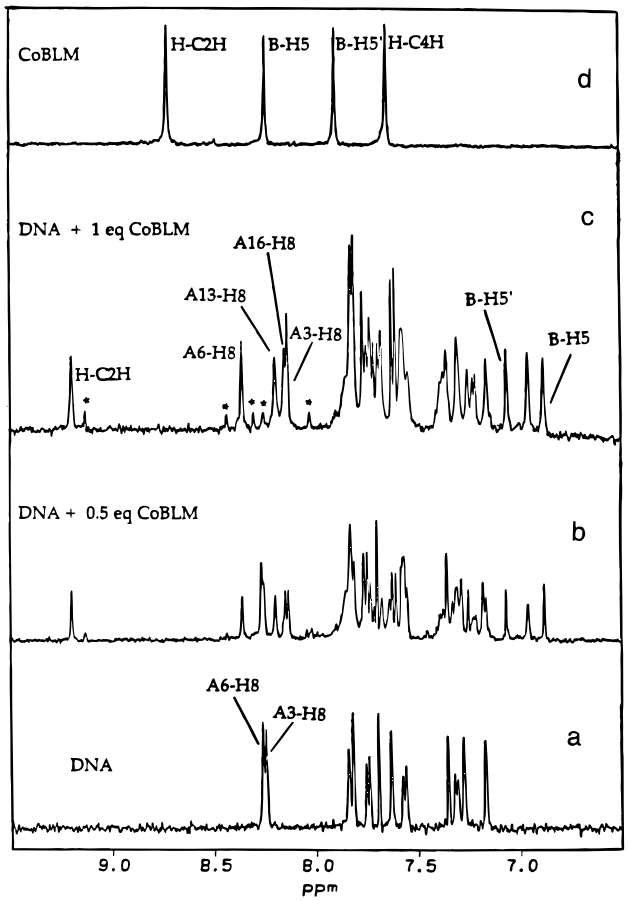

Figure 4. Titration of d(CCAGTACTGG) (**2**) with CoBLM A2 green at 20 °C. Downfield region of the ^{1}H NMR: CoBLM in 50 mM sodium phosphate (pH 6.8) and decameric duplex DNA (2.0 mM) in 50 mM sodium phosphate (pH 6.8) with 0, 0.5, and 1 equiv of CoBLM added. Asterisks indicate the presence of a minor complex.

shown), the CH_3 groups of T5 (1.38 ppm) and T8 (1.59 ppm) in free DNA decrease in magnitude upon addition of CoBLM and four new methyl resonances at 1.57 ppm (T8), 1.19 ppm (T15), 1.55 ppm (T18), and 1.45 ppm (T5) appear. In addition, the CH_3 group of the pyrimidine moiety in CoBLM (Figure 1) shifts downfield from 2.48 to 2.67 ppm. Finally, heteronuclear ^{1}H−^{13}C NMR experiments, discussed subsequently, reveal upfield shifts of the bithiazole H5 and H5′ protons from 8.21 to 6.87 ppm and 7.87 to 7.04 ppm, respectively, when CoBLM binds to the duplex (Figure 4). These observations are reminiscent of our previous studies with d(CCAGGCCTGG)[16] and suggest that the drug binds via partial intercalation of its bithiazole tail. In addition, a minor complex (Figure 4, resonances with *), accounting for 20% of the total DNA, is also apparent.

^{1}H and ^{13}C Assignments of CoBLM A2 Green. The assignments of the ^{13}C chemical shifts of the bithiazole moiety of CoBLM A2 green and of the ^{1}H and ^{13}C chemical shifts of its sugars have played a key role in distinguishing between various models for the structure of CoBLM A2 green and its structure bound to DNA of defined sequence.[48] The strategy for proton assignments in CoBLM A2 green is similar to that previously reported by Akkerman et al. for the assignments of ZnBLM and FeBLM-CO.[50,51] Furthermore, the proton assignments of a mixture of CoBLMs A2 (green and brown forms) were recently reported by Xu et al.[28] Our assignments of the proton chemical shifts of CoBLM A2 green at 5 °C, pH 6.8,

(47) Heinemann, U.; Alings, C. *J. Mol. Biol.* **1989**, *210*, 369−381.
(48) Wu, W.; Vanderwall, D. E.; Turner, C. J.; Kozarich, J. W.; Stubbe, J. *J. Am. Chem. Soc.* **1996**, *118*, 1281−1294. (following paper in this issue).
(49) Absalon, M. J.; Stubbe, J.; Kozarich, J. W. *Biochemistry* **1995**, *34*, 2065−2075. (b) Absalon, M. J.; Wu, W.; Stubbe, J.; Kozarich, J. W. *Biochemistry* **1995**, *34*, 2076−2086.
(50) Akkerman, M. A. J.; Haasnoot, C. A. G.; Hilbers, C. W. *Eur. J. Biochem.* **1988**, *173*, 211−225.
(51) Akkerman, M. A. J.; Neijman, E. W. J. F.; Wijmenga, S. S.; Hilbers, C. W.; Bermel, W. *J. Am. Chem. Soc.* **1990**, *112*, 7462−7474.

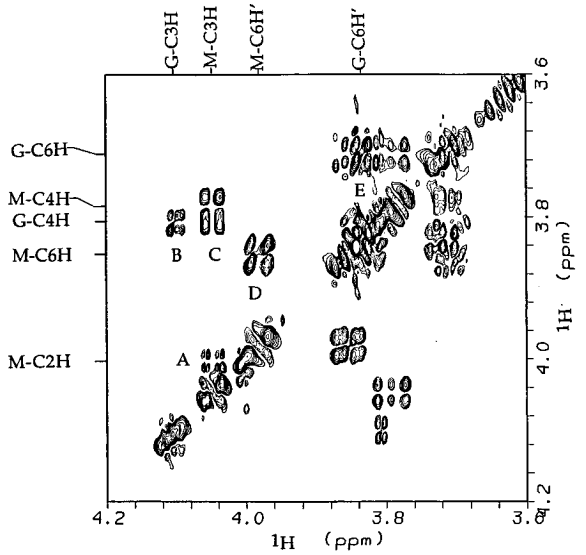

Figure 5. Expanded P.E. COSY spectrum of the sugar region in D_2O at 5 °C, pH 6.8. Peak assignments are (A) M-C2H (4.00 ppm) to M-C3H (4.05 ppm); (B) G-C3H (4.10 ppm) to G-C4H (3.80 ppm); (C) M-C3H (4.05 ppm) to M-C4H (3.78 ppm); (D) M-C6H (3.85 ppm) to M-C6H′ (3.98 ppm); (E) G-C6H (3.71 ppm) to G-C6H′ (3.84 ppm).

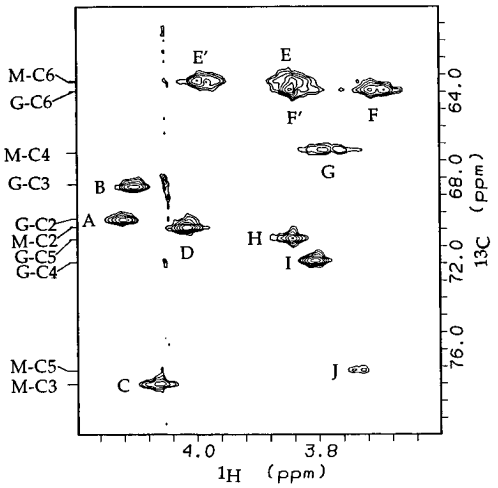

Figure 6. Expanded HMQC spectrum of the sugar region in D_2O at 5 °C, pH 6.8. Peak assignments (proton chemical shift in ppm, carbon chemical shift in ppm) are (A) G-2 (4.11, 69.9); (B) G-3 (4.10, 68.4); (C) M-3 (4.05, 77.6); (D) M-2 (4.00, 70.3); (E and E′). M-6 (3.85/3.98, 63.5); (F and F′) G-6 (3.71/3.84, 63.9); (G) M-4 (3.78, 66.7); (H) G-5 (3.84, 70.8); (I) G-4 (3.80, 71.8); (J) M-5 (3.84, 70.8).

are in most cases within ±0.05 ppm of those reported by Xu et al. at −5 °C, pH 7.4 (see table in supplementary information, differences are underlined). The availability of homogeneous CoBLM A2 green, however, has allowed the assignment of all sugar proton resonances of gulose and mannose and all carbon resonances of CoBLM. This unique information has allowed us to define the chirality of the cobalt as well as the nature of the axial ligands of CoBLM A2 green.

Assignment of the Proton Chemical Shifts of Gulose and Mannose. Heteronuclear $^1H-^{13}C$ NMR methods, HMQC and HMBC, played an essential role in the completion of the sugar assignments. The HMQC spectrum allowed identification of the gulose and mannose anomeric C/H cross peaks, as the characteristic anomeric carbon chemical shifts between 80 and 100 ppm are well separated from the rest of the sugar carbon resonances. The G-C1H can be distinguished from the M-C1H in the HMBC spectrum as two unique cross peaks are observed between the H-CβH and the G-C1 and between the H-Cβ and the G-C1H. With the chemical shifts of G-C1H and M-C1H established, the assignments of the G-C2H, M-C2H, M-C3H, and M-C4H are straightforward from the P.E. COSY spectrum (for M-C2H, M-C3H, and M-C4H, see A and C, Figure 5). The assignment of the M-C3H has proven to be an important piece of information for distinguishing between the structures of several alternative CoBLM A2 green isomers. Acquisition of the HMQC spectrum provided dispersion in the carbon dimension sufficient to spread out all the sugar C/H cross peaks for identification of the chemical shifts of the remaining protons. The H6 and H6′ sugar protons are distinctive, as each C6 carbon exhibits cross peak patterns to two protons (see E, E′ and F, F′, Figure 6). Corroboratively, large COSY cross peaks are observed between these geminal methylene protons (see D and E, Figure 5). The M-C6 carbon can be distinguished from the G-C6 carbon by a cross peak in the HMBC spectrum between the carbon resonance at 63.5 ppm (M-C6) and the proton resonance at 3.78 ppm (M-C4H). The assignment of the M-C4H allowed the chemical shift assignment of M-C5H. The M-C4H in the HMBC spectrum shows a cross peak to the M-C5 at 77.0 ppm, allowing the assignment of the M-C5H by the HMQC method. Thus, the assignments of the mannose carbon and proton chemical shifts are complete.

The assignments of the carbon and proton chemical shifts of C-3, C-4, and C-5 of gulose have been more problematic. The G-C/H3 chemical shifts were initially assigned from the HMQC spectrum (B, Figure 6, Table 1). The chemical shift of G-C3H (4.10 ppm) and its similarity to that of G-C2H (4.11 ppm) provides an explanation for the inability to detect connectivity in the P.E. COSY spectrum; it is too close to the diagonal (Figure 5). Further support for the assignment of G-C3 comes from its cross peak to G-C1H in the HMBC spectrum, and from this assignment, the G-C4H can be readily identified from the P.E. COSY spectrum (B, Figure 5). Identification of the G-C4H allowed the assignment of G-C4. Finally the only remaining unassigned carbon in the HMQC spectrum is G-C5, which then allowed the identification of the G-C5H. The G-C5H shows a cross peak with G-C6 in the HMBC spectrum, confirming this assignment. The results of these assignments are summarized in the supporting information and Table 1.

Assignment of the Carbon Chemical Shifts in CoBLM A2 Green. Using the complementary HMQC and HMBC methods, all of the ^{13}C assignments were successfully completed.[52] Essential to understanding the mode of binding of the bithiazole moiety in the drug−DNA complex is distinguishing between the B-C5′ and B-C5. These assignments allowed the unambiguous identification of the B-C5′H and B-C5H resonances. The HMBC method can assign the bithiazole quaternary carbons as B-C2′ shows cross peaks to the B-CαH and B-CβH as well as to B-C5′H, while B-C2 has cross peaks to B-C5′H and B-C5H. B-C4′ and B-C4 are assigned on the basis of their single cross peak to the B-C5′H and B-C5H, respectively. Thus, the B-C5H and B-C5′H can be assigned to 8.17 and 7.82 ppm in CoBLM A2 green and their upfield shifts when bound to duplex DNA have been monitored using the HMQC method.

Assignment of the Exchangeable Protons of CoBLM A2 Green. The assignment of exchangeable protons of metallo-BLMs by NOESY experiments carried out in H_2O has previ-

(52) There are two exceptions. A distinction could not be made between the amide carbonyl carbons of the P and H moieties as both of them have cross peaks to the H-CαH proton and neither show cross peaks to the H-CβH proton. Previous studies of Akkerman et al. permitted assignment of these two resonances in the FeBLM-CO based on an observed cross peak to the H−CβH.[51] Assignments reported in Table 1 for these two carbonyls are based on the relative chemical shifts and previous assignments and should be considered tentative.

Table 1. Comparison of Proton Chemical Shifts (ppm) of Apo- and Metallo-BLMs

carbons		apo[a] (297 K, pH 7)	Zn[a] (277 K, pH 7)	Fe[a] (277 K, pH 7)	Co[b] (278 K, pH 6.8)	carbons		apo[a] (297 K, pH 7)	Zn[a] (277 K, pH 7)	Fe[a] (277 K, pH 7)	Co[b] (278 K, pH 6.8)
P	Cα	40.6	33.9	34.1	35.5		C═O	172.4	172.2	172.4	174.7
	Cβ	60.1	56.1	64.0	65.1	B	Cα	32.4	32.4	32.5	35.5
	CH_3	11.2	11.1	10.0	12.0		Cβ	39.4	39.6	39.5	41.9
	C2	165.7	161.6	167.5	171.5		C5	125.5	125.5	126.0	127.5
	C4	165.0	168.0	166.4	169.4		C5′	119.4	119.5	119.6	121.3
	C5	112.6	114.2	117.2	119.9		C4	149.1	149.1	149.4	151.2
	C6	152.5	148.4	153.1	152.9		C4′	147.3	147.3	147.3	149.9
	HNC═O	168.0	169.3	173.1	176.7		C2	163.0	163.1	163.6	165.3
	H_2NC═O	176.5	176.6	175.4	177.3		C2′	170.9	171.0	171.5	173.8
H	Cα	57.3	61.1	55.6	60.1		C═O	163.7	163.7	164.0	165.8
	Cβ	73.4	70.6	69.2	71.7	S	Cα	41.3	41.3	41.3	43.4
	C2	137.3	137.8	142.2	144.8		Cβ	24.0	24.0	24.1	26.6
	C4	118.0	118.2	119.8	122.2		Cγ	38.0	38.0	38.1	40.3
	C5	135.2	135.5	135.9	136.0		$(CH_3)_2$	25.1	25.1	25.1	27.3
	C═O	169.4	172.0	170.0	173.6	G	C1	97.8	95.6	94.9	97.4
A	Cα	53.0	52.5	55.9	59.3		C2	70.6	68.3	68.1	69.9
	Cβ	47.8	45.0	49.4	51.8		C3	68.2	66.6	66.6	68.4
	C═O	172.3	173.8	173.4	173.6		C4	69.5	70.1	69.7	71.8
V	αCH_3	12.3	12.1	13.2	9.8		C5	67.4	67.7	68.1	70.8
	γCH_3	15.1	15.0	14.3	20.4		C6	60.6	61.6	61.6	63.9
	Cα	43.0	43.0	43.4	42.9	M	C1	98.5	97.2	96.7	98.5
	Cβ	74.7	74.7	74.4	77.7		C2	68.7	68.3	68.1	70.3
	Cγ	47.9	47.3	47.8	49.6		C3	74.7	75.5	75.3	77.6
	C═O	177.8	177.6	177.8	179.9		C4	65.1	64.5	64.7	66.7
T	CH_3	19.3	19.3	19.3	22.4		C5	73.9	74.7	74.6	77.0
	Cα	59.5	59.7	59.7	60.0		C6	61.3	61.3	61.4	63.5
T	Cβ	67.4	67.4	67.3	72.4		C═O	158.3	157.7	157.8	160.2

[a] Akkerman et al.[51] [b] This study, 50 mM phosphate buffer.

ously provided important information about the ligands coordinated to ZnBLM and FeBLM-CO,[50,51] and thus, we have undertaken to make these assignments for CoBLM A2 green. The secondary amine proton of β-aminoalanine (A-NH) and all but one of the secondary amide protons were readily assigned by standard methods (see table in supporting information). As in the case of previous metallo-BLMs, the secondary amide hydrogen of the β-hydroxyhistidine moiety was not detected. This is consistent with previously published data[50,51] that strongly suggest that this amide is deprotonated and is a ligand to the cobalt. In the case of the ZnBLM and FeBLM-CO, four additional sets of exchangeable, paired protons have been reported. Two have been assigned to the primary amides of the β-aminoalanine (A) and the pyrimidinylpropionamide (P) moieties. A third has been assigned to the primary amine of A due to an NOE with A-CαH and the fourth to the carbamoyl group of mannose on the basis of their rapid exchange with H_2O. In the case of CoBLM A2 green, only two of the four sets of protons have been detected in the NOESY spectra in H_2O. Studies in which the pH is lowered to minimize the exchange rate are not possible with CoBLM as it is chemically unstable under acidic conditions. The pairs of exchangeable proton resonances observed with CoBLM A2 green have chemical shifts at 8.08/7.32 and 6.76/6.18 ppm and exhibit strong NOEs to each other, but not to any other protons; therefore, assignment of these protons was not possible. Furthermore, no protons assignable to the primary amine of β-aminoalanine have been detected. Finally, a pair of exchangeable proton resonances at 7.73 and 7.94 ppm have been assigned to the 4-amino protons of the pyrimidine by virtue of their NOEs to each other and to the P-CH_3. This assignment is important as one of these protons plays a key role in binding of CoBLM A2 green to DNA, as described in the accompanying paper.[48]

NOE and Dihedral Angle Constraints. An essential step in defining the screw sense and the ligation state of CoBLM A2 green, and ultimately its structure, is to obtain distance and dihedral angle constraints from the NMR data. The assignments of all the ^1H and ^{13}C chemical shifts have allowed us to determine 55 nontrivial NOEs for use as distance constraints, as shown in Table 2. These data can be compared with the NOE constraints previously reported by Xu et al. and with those of Akkerman et al. for the FeBLM-CO and ZnBLM complexes[50,51] (Table 2).

Analysis of the coupling constants for the H, A, P, T, and V moieties (Table 3) allowed for the incorporation of eight dihedral angle constraints for use in molecular modeling. Additionally, the coupling constants for H1 and H2 of the sugars G and M (Table 3) and the previous calculations of these coupling constants by Akkerman et al.[50] for the two chair conformations have allowed us to assume the chair conformations shown in Figure 1. Only limited information on the coupling constants of the other metallo-BLMs has previously been reported in the literature. The additional structural definition provided by the dihedral angle constraints played an important role in identification of the axial ligands and the refinement of our model.

Previous Model Building Studies. Xu et al.[28] have recently reported the first 2D NMR studies on CoBLMs and proposed, on the basis of their NOE constraints and molecular modeling, two models for A2 green: A and B (our versions of their structures are shown in Figure 7a,c). They made several assumptions to arrive at these models. They assumed that the secondary amine of A, the N1 of P, the deprotonated amide of H, and the N_δ of H (Figure 1, N's) are equatorial ligands to cobalt and that one of the axial ligands is a hydroperoxide. These assumptions are consistent with biophysical studies by many investigators.[53] They also assumed that the second axial ligand is provided by the primary amino group of A. In the case of both ZnBLM and FeBLM-CO, however, previous workers have interpreted their 2D NMR studies to indicate that an axial ligand is provided by the carbamoyl nitrogen of mannose.[50,51] This

(53) (a) Dabrowiak, J. C.; Tsukayama, M. *J. Am. Chem. Soc.* **1981**, *103*, 7543−7550. (b) Dabrowiak, J. C. in *Advanced Inorganic Biochemistry*; Eichhorn, G. L., Marzilli, L. G., Eds.; Elsevier Biomedical: New York, 1982; Vol. 4, pp 69−113.

Table 2. Comparison of NOEs in Metallo-BLMs[e]

CoBLM A2 green[a] mixing time (200 ms)	size	CoBLM[b] (300 ms)	FeBLM-CO[c] (400 ms)	ZnBLM[d] (400 ms)	CoBLM A2 green[a] mixing time (200 ms)	size	CoBLM[b] (300 ms)	FeBLM-CO[c] (400 ms)	ZnBLM[d] (400 ms)
H-C2H- - -A-CβH′	m	y	y		G-C1H- - -M-C5H	m		y	y
H-C2H- - -A-CβH	w		y		G-C1H- - -G-C6H	w			
A-CβH- - -P-CαH′	m		y	y	G-C1H- - -G-C4H	w			
P-CβH- - -A-CβH	w		y	y	G-C1H- - -M-C2H	w			
H-C2H- - -A-NH	m	y	y	y	H-CαH- - -G-C6H	w			
H-C2H- - -P-CβH	w		y		H-CαH- - -M-C5H	m			y
H-C2H- - -T-CH_3	s	y			H-CαH- - -M-C3H	w			
H-C2H- - -T-CβH	w				M-C1H- - -G-C2H	s			y
H-C2H- - -T-CαH	w				M-C1H- - -G-C3H	s			y
H-C2H- - -T-NH	w				M-C1H- - -G-C4H	w			
H-C2H- - -V-CαH	m	y			T-CαH- - -T-CH_3	m	y	y	
H-C2H- - -V-αCH_3	w	y			V-αCH_3- - -V-CγH	s	y		
H-C4H- - -V-CαH	w	y			V-γCH_3- - -V-CβH	s	y		
H-C4H- - -V-αCH_3	m	y		y	V-αCH_3- - -V-CβH	m	y	y	
P-CβH- - -T-CβH	w				B-NH- - -T-CαH	m	y	y	
H-C4H- - -H-CβH	s	y	y		B-NH- - -T-CβH	w	y	y	y
B-C5′H- - -V-CβH	m	y			B-NH- - -B-CαH	w			
B-C5′H- - -V-γCH_3	m	y			B-NH- - -B-CαH′	w			
B-C5H- - -P-CH_3	m	y			T-NH- - -V-αCH_3	w	y	y	y
G-C1H- - -H-CβH	s	y			V-NH- - -V-CβH	s	y	y	y
H-CαH- - -G-C1H	s		y	y	T-NH- - -V-CβH	m	y	y	y
M-C1H- - -G-C1H	w				T-NH- - -T-CH_3	w	y	y	
H-C4H- - -G-C5H	w		y	y	B-NH- - -T-CH_3	w	y	y	y
H-C4H- - -G-C6/6′H	w/w		y	y	V-NH- - -V-CαH	m		y	y
H-CβH- - -G-C6H	w				V-NH- - -V-γCH_3	m	y	y	y
H-CβH- - -G-C4H	w				T-NH- - -V-CαH	m	y	y	y
H-CβH- - -G-C2H	w	y			T-NH- - -V-γCH_3	m			y

[a] This study. [b] Xu et al.[28] [c,d] Akkerman et al.[50,51] [e] w, m, s: weak, medium, strong NOE. y: observed.

Table 3. Comparison of Coupling Constants (Hz) in Metallo-BLMs

protons	CoBLM A2 green[a]	FeBLM-CO[b]	ZnBLM[b]	apo-BLM[b]
H-CαH to H-CβH	2.7 ± 0.3	3.1 ± 0.2	3.1 ± 0.2	5.8 ± 0.2
G-C1H to G-C2H	3.9 ± 0.3		4.9	
P-CβH to P-CαH (3.20 ppm)	8.3 ± 0.3			
P-CβH to P-CαH′ (3.51 ppm)	4.6 ± 0.3			
T-CαH to T-CβH	2.9 ± 0.3			
M-C1H to M-C2H	1.2 ± 0.3		1.8	
T-NH to T-CαH	8.7 ± 0.3			
V-NH to V-CγH	7.9 ± 0.3			
A-NH to P-CβH	<3			
A-NH to A-CβH′ (3.22 ppm)	5 ± 2			
A-NH to A-CβH (2.74 ppm)	5 ± 2			
V-CαH to V-CβH	1.8 ± 1.2			
V-CβH to V-CγH	9.5 ± 1.2			
A-CβH′ (3.22 ppm) to A-CαH	3.0 ± 0.5	4.2 ± 0.2	2.0 ± 0.2	5.2 ± 0.2
A-CβH (2.74 ppm) to A-CαH	4.0 ± 1.2	7.2 ± 0.2	3.8 ± 0.2	7.2 ± 0.2

[a] This study, 50 mM phosphate, pH 6.8, at 5 °C. [b] Akkerman et al.[51]

ligation state was not considered as an option in the models proposed by Xu et al. Finally, Xu et al. favored the A form (Figure 7a) over the B form (Figure 7c) on the basis of their relative energetics, although they were unable to distinguish between these structures with their NMR data.[28]

Solution Structure of CoBLM A2 Green. On the basis of previous studies on chelation to cobalt[53] and the ambiguity in the axial ligation state, we have initially considered four theoretically possible structures, I, II, III, and IV in Figure 7, parts a, b, c, and d, respectively. These four structures reflect the two alternative screw senses which define the stereochemistry of ligand arrangement around the metal and the two possible axial ligands, either the primary amine of A or carbamoyl nitrogen of M, for each of the screw sense isomers. Structures I and II have the same screw sense, while structures III and IV have the opposite screw sense. Structures I and III contain the primary amine of A as the axial ligand, while structures II and IV have the carbamoyl nitrogen of M at that position. In the discussion that follows, arguments will be made on the basis of our NMR data that only structure I, which contains a primary amine of A as the axial ligand, meets all of the constraints. In addition, our data will be compared and contrasted with previous 2D NMR information on the ZnBLM and FeBLM-CO complexes.

Using the dihedral angle and NOE constraints, we have built models of the four isomers discussed above. The easiest models to eliminate are structures III and IV. Structure IV with a carbamoyl axial ligand (Figure 7d) can be eliminated as a significant number of NOE constraints are violated. These specifically include the NOEs between the H and V residues and those between the H-CαH and sugar protons.[54] Furthermore, this structure requires a trans configuration between the H-CαH and the H-CβH which is inconsistent with the small coupling constant observed (2.7 Hz, Table 3). These problems and the extremely high CHARMm potential energy in comparison with structures I and II (Table 4) allow us to eliminate this model.

Structure III with the primary amine of A as a ligand is the B conformation proposed by Xu et al. for CoBLM A2 green. Our molecular dynamics calculations also suggest that this model is of higher energy than that of structure I (Table 4) and, in general, does not satisfy the experimentally derived constraints. Additionally, if all of the NOEs and the dihedral angle constraints are satisfied, the model predicts that the V, T, and B moieties of CoBLM A2 green must be located on the same side and in close contact to the primary amine ligand (Figure 7c). This location requires the existence of a number of NOEs

(54) Most noticeably, NOEs between H-C4H and V-αCH_3, H-CαH and G-C1H, H-CαH and G-C6/6′H, and H-CαH and M-C5H are all violated by more than 0.6 Å.

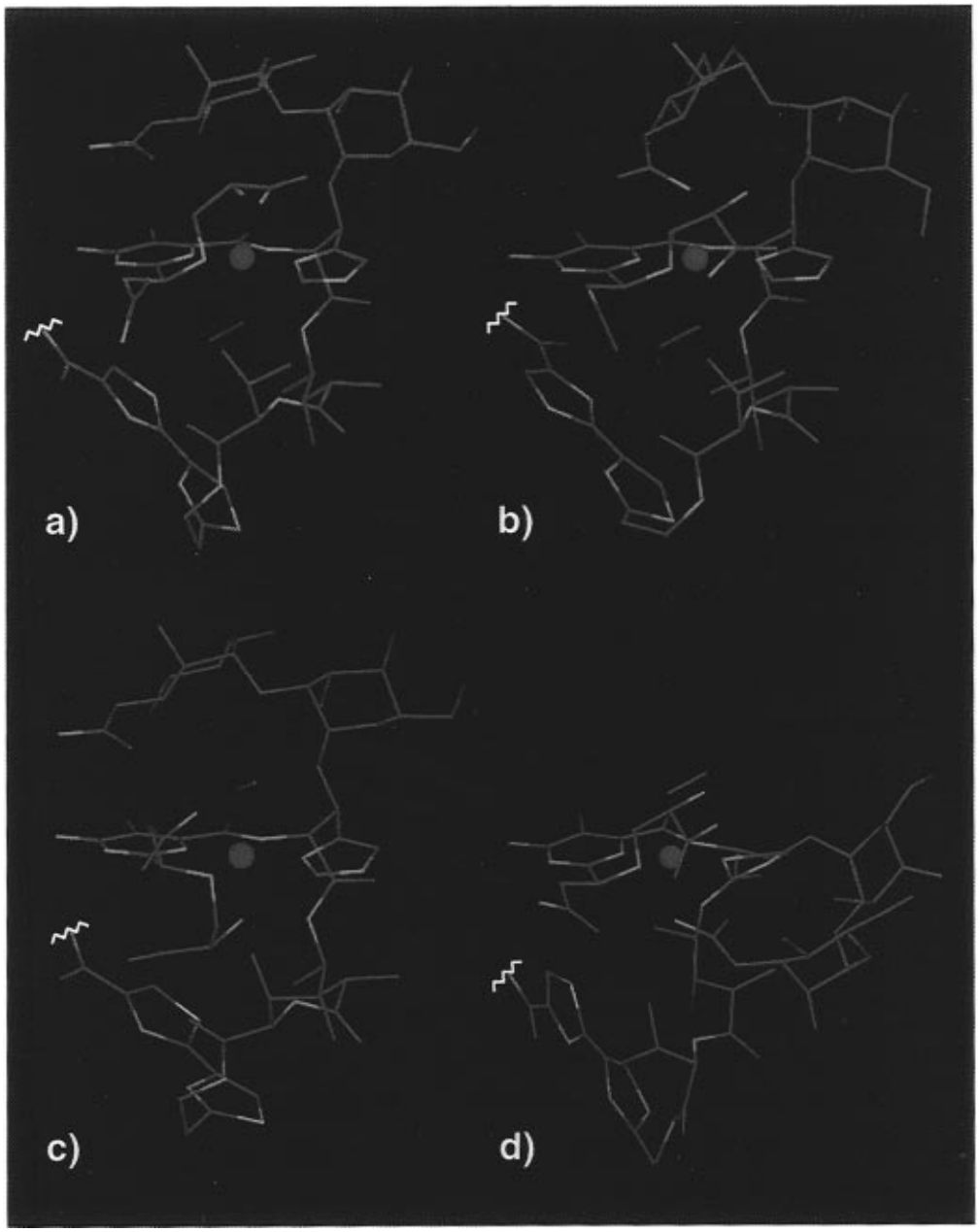

Figure 7. Four isomers of CoBLM A2 green: same screw sense isomers (a) structure I with primary amine of A or (b) structure II with carbamoyl nitrogen of M as an axial ligand; and the opposite screw sense isomers (c) structure III with the primary amine of A or (d) structure IV with carbamoyl nitrogen of M as an axial ligand. The sulfonium tail has been excluded from the figure for clarity.

between the A spin system and the V and T spin systems that would be easily detected, such as A-CαH to V-CβH (strong), A-CαH to V-CαH (medium), A-CβH to T-CβH (medium), and A-CαH to V-CβH (medium). None of these NOEs are observed, thereby eliminating this isomer, a variant of structure B of Xu et al.,[28] from further consideration. Finally, as described in the accompanying paper, neither of these isomers (structures III and IV) can bind to DNA and successfully satisfy the wealth of NMR information available on the DNA−drug complex.

Energy-minimized models for the other screw sense isomers, structures I and II with the primary amine of A and the carbamoyl of M as the axial ligand, respectively, are shown in Figure 7, parts a and b, and in more detail in Figure 8, parts a and b. In contrast to the screw sense isomers discussed above, in the structures I and II, the peptide linker region and the bithiazole moiety are located on the bottom face of the metal plane, sharing the same face with the hydroperoxide ligand. The possible axial ligands both reside on the top face of the metal plane, which makes differences between the two structures rather subtle. In fact, both the primary amine and carbamoyl group can be interchanged as axial ligands with relatively minor structural reorganization of CoBLM A2 green.

A number of considerations outlined subsequently have allowed us to favor the structure I with the primary amine of A as a ligand. One difference between the two, illustrated in Figure 8a,b, involves the M-C3H. Specifically, in the carbamoyl isomer, the M-C3H to H-CβH and to H-CαH are predicted to be strong and medium NOEs, respectively (Figure 8b). The alanine isomer predicts a weak and no NOE, respectively, which is the observed result (Figure 8a, Table 2). Thus, in the carbamoyl isomer, the M-C3H is closer to the H moiety, primarily due to the mannose group being restricted to the ligation sphere of cobalt.

Examination of the coupling constants between the α and β protons of A has provided additional support for the structure shown in Figure 8a. These coupling constants have been previously used by Akkerman et al. studying ZnBLM and

Table 4. Structure and Energy Statistics from Molecular Dynamics Calculations

	structure I		structure II		structure III		structure IV	
	all structures	final av structure[a]	all structures	final av structure	all structures	final av structure	all structures	final av structure
rmsd from distance restraints (Å)	0.0100 ± 0.0026	0.0093	0.0147 ± 0.0045	0.0480	0.0859 ± 0.0440	0.0641	0.2003 ± 0.0034	0.2064
potential energy terms[a]								
total	98.2 ± 3.5	95.9	128.0 ± 3.4	124.0	118.0 ± 0.9	120.0	467.0 ± 1.4	473.0
NOE constraint	0.176 ± 0.093	0.144	0.420 ± 0.084	0.437	4.33 ± 0.69	4.80	66.6 ± 1.8	70.4
dihedral constraint	1.04 ± 0.07	1.14	1.52 ± 0.36	1.50	2.47 ± 0.62	2.04	20.9 ± 0.5	22.0
van der Waals	−70.1 ± 2.1	−72.9	−62.8 ± 1.9	−63.7	−61.3 ± 1.1	−61.3	11.7 ± 1.9	14.4
bond	5.93 ± 0.13	5.80	8.71 ± 0.36	8.63	6.55 ± 0.12	6.03	24.7 ± 0.4	19.5
angle	93.7 ± 1.4	94.4	108.0 ± 0.8	107.0	97.7 ± 0.5	97.8	220.0 ± 4.5	221.0
dihedral angle	64.3 ± 1.7	64.7	68.8 ± 1.0	66.1	67.4 ± 0.6	67.5	111.0 ± 1.0	112.0
improper angle	3.19 ± 0.11	2.61	3.25 ± 0.06	3.70	2.77 ± 0.29	2.86	12.5 ± 1.6	13.8
atomic rmsd for all atoms (Å)	0.7680	0.7709[d]	0.7542	0.9854	0.5216	0.6828	0.5672	0.7239

[a] The coordinates of the final structures of the individual molecular dynamics calculations, averaged, and minimized. [b] Energy terms in kcal mol^{-1}. [c] Because of the expected disorder and lack of NOES to the sulfonium tail and the possibility of either a cis or trans orientation of the thiazolium rings of the bithiazole, these moieties were not included in the rms calculation. [d] All structures vs the final average structure.

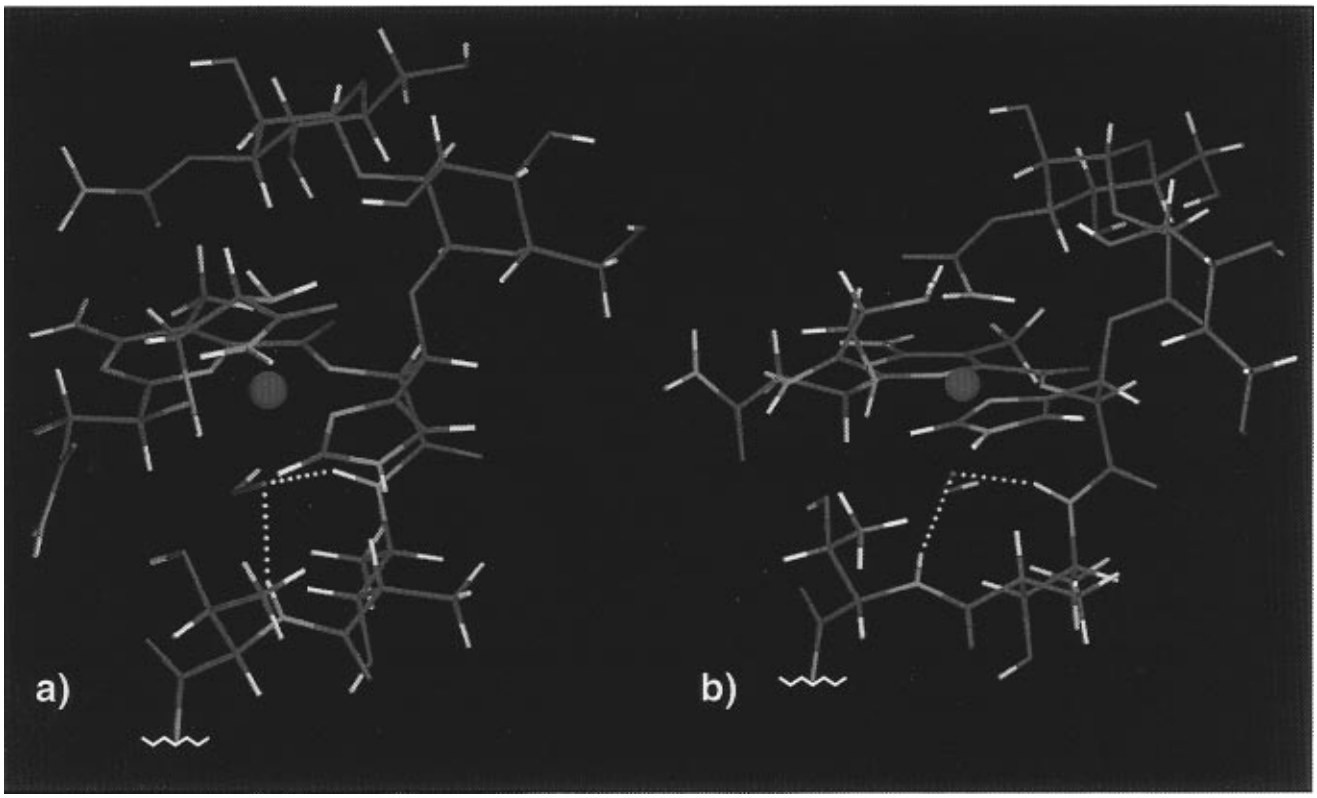

Figure 8. Two isomers of CoBLM A2 green (same screw sense): (a) structure I with the primary amine of A or (b) structure II with carbamoyl nitrogen of M as an axial ligand. The two structures are shown in slightly different orientations to provide the optimal view of the axial nitrogen ligand in each case, and the bithiazole and sulfonium moieties have both been excluded (zigzagged line).

FeBLM-CO as predictors of whether the primary amine of A is actually an axial ligand in these complexes.[50,51] In apo-BLM, the coupling constants between the α and β protons of A (7.2 and 5.2 Hz, Table 3) are indicative of rapidly interconverting conformations. Similar sizes of these coupling constants (7.2 Hz and 4.2 Hz) have been reported for the FeBLM-CO and have been interpreted to indicate that the primary amine is not an axial ligand in this complex. In ZnBLM, however, the coupling constants (3.8 and 2.0 Hz) are substantially different from those observed with apo-BLM. These values have been interpreted to suggest that, in this complex, the primary amine is a ligand and that it is constrained to a gauche−gauche conformation of the Cα−Cβ bond. The values of coupling constants in the A moiety of CoBLM A2 green (3.0 and 4.0 Hz) and the calculated rotamer population of the Cα−Cβ bond are also indicative of a gauche−gauche conformation (>80%) and support the hypothesis that the primary amine is an axial ligand in this complex as well. Finally, the line widths of the A-CαH and A-CβH are slightly larger than the rest of the protons of the CoBLM A2 green, suggestive of a local movement of the Cα−Cβ bond within this ligation state.

NOE patterns observed for the H-C2H to the A-CαH and A-CβHs are also consistent with the primary amine as the axial ligand of CoBLM A2 green, although the conclusions must be drawn cautiously. With the carbamoyl group as a ligand, medium and weak to medium NOEs are predicted between H-C2H to A-CαH and to A-CβHs, respectively. With the primary amine as an axial ligand, weak to medium NOEs are also predicted from H-C2H to A-CβHs. However, the NOE between H-C2H to A-CαH is predicted to be very weak. Weak to medium NOEs between the H-C2H to A-CβHs are observed in 200 ms mixing time NOESY spectrum. Only at 400 ms is an additional weak NOE observed between H-C2H and A-CαH consistent with the primary amine of A being an axial ligand.

A number of additional pieces of information support the primary amine ligation state (Figure 8a). The first is that studies with deglyco-BLM and more recently with demannosyl-BLM reveal that, despite the absence of the carbamoyl group, cleavage of DNA occurs with similar sequence selectivity and efficiency (approximately 30−50%) as the corresponding intact FeBLM.[22] These studies suggest that the carbamoyl group is not a ligand. Second, ample chemical precedent suggests that if cobalt has a choice between a primary amine and a carbamoyl nitrogen ligand, and there are no unusual geometrical constraints involved in the comparison of these options, the former is a more nucleophilic ligand and hence would be favored. Third, previous studies of Dabrowiak et al.[53] using the cobalt-containing pseudotetrapeptide A of BLM, a hydrolysis product of CoBLM A2 green, indicate that the primary amine can be a ligand to cobalt. Fourth, recent crystallographic studies of Tan et al. on CoPMAs, a series of CoBLM model compounds, also show that a primary amine group can be an axial ligand to cobalt.[37] Finally, the energy calculation using all available experimental distance and dihedral constraints reveals that structure I with the primary amine of A as the axial ligand is energetically more favorable in all aspects of potential energy terms, when compared with structure II with the carbamoyl nitrogen of M as the axial ligand (Table 4). This information, in addition to the model studies and the analysis of NOEs and coupling constants presented above, allows us to favor structure I with the amino group of A as the axial ligand as the structure of CoBLM A2 green.

Comparison of CoBLM A2 Green with Other Metallo-BLMs. The structures of ZnBLM and FeBLM-CO, based on 2D NMR analysis, have previously been reported by Akkerman et al.[50,51] In the case of FeBLM-CO, the axial ligand has been proposed to be the carbamoyl group, and in the case of ZnBLM, the axial ligands have been proposed to be the carbamoyl of M and the primary amine of A.[50,51] The equatorial ligands in all metallo-BLMs are noncontroversial. The idea of a screw sense isomer has not been previously considered with these complexes.

The most conspicuous differences between the CoBLM A2 green and its Zn and Fe counterparts result from the observation of unique long-range NOEs between the B-H5 and the P-CH_3 and the B-H5′ and the V moiety in the case of CoBLM A2 green (see Table 2, and parts D, E, and F in the figure in supporting information). These NOEs are identical to those previously reported by Xu et al.[28] and, as described above, allowed them to propose a compact model for CoBLM A2 green in which the bithiazole tail is folded back underneath the equatorial plane of the metal binding domain[28] (Figure 7a). These NOEs have not previously been detected in the cases of FeBLM-CO and ZnBLM, and as a consequence, the bithiazole tail has been ignored in the molecular modeling of these structures. The resulting proximity of the pyrimidine to the penultimate thiazolium ring in CoBLM A2 green (Figure 7a and 8a) is presumably responsible for the inequivalence of the chemical shifts of the two P-NH_2 protons (Figure 1 and supporting information). These two protons are degenerate in both ZnBLM and FeBLM-CO complexes.

A second major difference between the CoBLM A2 green and the other metallo-BLMs is that the conformations of V and T linker regions are well defined. The coupling constants in the V and T moieties of CoBLM A2 green placed constraints on four out of the six backbone dihedral angles (Table 3). As a result, the dihedral angles[55] in the final structure give rise to a turn that maintains the peptide linker region underneath the metal coordination plane (Figure 8a). This conformation provides an explanation for a number of initially puzzling observations made by NMR concerning this linker region. The chemical shifts of the V-αCH_3 and V-CαH are dramatically upfield shifted in CoBLM A2 green in comparison with the apo-BLM, ZnBLM and FeBLM-CO complexes. Specifically, a comparison between the apo-BLM and CoBLM reveals a shift from 1.10 to 0.62 ppm for V-αCH_3 and 2.45 to 0.94 ppm for V-CαH. The structure reveals that both the V-αCH_3 and the V-CαH are positioned directly underneath the imidazole ring of H whose ring current causes shielding and hence large upfield shifts. Examination of the NOESY spectrum of CoBLM A2 green reveals that both V-αCH_3 and V-CαH show NOEs to H-C2H and H-C4H of the imidazole ring (Figure 8a, Table 3), consistent with this constrained structure. A similar trend in the chemical shifts is also observed with ZnBLM, but with much smaller upfield changes (supporting information). Examination of the NOE patterns for ZnBLM reveals that, unlike the CoBLM A2 green, only an NOE from H-C4H to V-αCH_3 is reported. In complete contrast, the FeBLM-CO complex shows no unusual chemical shifts of the V-CαH and V-αCH_3 and no NOEs from imidazole protons to the valeryl protons are reported.

These structural differences raise an interesting question as to why the CoBLM A2 green adopts this well-defined compact structure in the peptide linker region. In structure I, with the primary amine of A as a ligand (Figure 8a), the amide protons of the V and T moieties are well positioned to form hydrogen bonds with the proximal oxygen of the hydroperoxide ligand,[56] which could stabilize the observed conformation. This hypothesis is supported by the large downfield chemical shift changes (∼1 ppm) of the V-NH and T-NH relative to those observed in ZnBLM and FeBLM-CO (supporting information).

How good a model is CoBLM A2 green for activated BLM? Unfortunately, the only direct comparison that can be made is to FeBLM-CO, in which the metal is in the 2+ oxidation state and possesses a CO ligand in place of a hydroperoxide anion ligand. In the FeBLM-CO complex of Akkerman et al., the second axial ligand is proposed to be provided by the carbamoyl group.[51] The evidence in support of this assignment is based on the 0.54 ppm upfield chemical shift of the M-C3H relative to its chemical shift in apo-BLM. However, with CoBLM A2 green, we see an even larger upfield chemical shift change for this proton (0.63 ppm) and we have now established that the carbamoyl group is not a ligand in CoBLM A2 green. Thus, the chemical shift argument does not provide strong support for their conclusion concerning axial ligation. Their second argument in favor of the carbamoyl ligand was that the two protons of this ligand were nonequivalent and distinguishable, thus suggesting ligation to iron. However, the assignment of these protons is based solely on the argument that they are the protons most rapidly exchanging with H_2O. This tentative assignment, the fact that amines are better ligands than carbamoyl groups when all other factors are equivalent, leads us to suggest that the primary amine of A could be an axial ligand in FeBLM-CO as in the CoBLM A2 green case. To account for the large coupling constants between the A-CαH and A-CβHs in the FeBLM-CO complex, one, then, could propose that the ligand can undergo exchange on the NMR time scale.[57] Regardless of the structure of the FeBLM-CO complex, it is

(55) Backbone angles are H−CO, V−N ,V−Cγ, V−Cβ =118°; V−N, V−Cγ, V−Cβ, V−Cα = −59°; V−Cγ, V−Cβ, V−Cα, V−CO = 178°; V−Cβ, V−Cα. V−CO, T−N = −68°; V−CO, T−N, T−Cα, T−CO = −122°; T−N, T−Cα, T−CO, B−N =120°.

(56) V-NH to O distance = 2.1 Å, N−H- - -O angle = 126°; T-NH to O distance = 2.3 Å, N−H- - -O angle = 161°. Note that no hydrogen bond or electrostatic terms were included in any structure calculations.

(57) Lippard, S. J.; Berg, J. M. *Principles of Bioinorganic Chemistry*; University Science Books: Mill Valley, CA, 1994; pp 28−29. (b) Basolo, F.; Pearson, R. G. *Mechanisms of Inorganic Reactions*; John Wiley & Sons, Inc.: New York, 1967; pp 124−246.

not unreasonable to assume in the $Fe^{3+}OOH$ complex that the primary amine of A is a ligand. Further analysis of this problem using ^{15}N-labeled β-aminoalanine is warranted and should be readily accessible given the recent user-friendly synthesis of BLM by Boger's group.[58] On the basis of these arguments, we believe that the isomer with the primary amine of A as an axial ligand is an excellent model for activated BLM.

Choice of Oligonucleotide Sequence for Examination of the Structure of CoBLM A2 Green Bound to DNA. The final prerequisite for defining the basis of molecular recognition between CoBLM A2 green and DNA is the choice of an appropriate oligonucleotide. Our recently reported preliminary studies have shown that CoBLM A2 green forms a 1:1 complex with d(CCAGGCCTGG)[16] and has led to a solution structure of the complex described in the accompanying paper.[48] We have shown herein that there is a single cleavage site (C6) in this duplex as predicted (Figure 3), and furthermore, studies monitoring the fluorescence quenching have allowed the determination of a single binding site with an apparent K_d of 10^{-7} M. As indicated in our preliminary studies and defined in detail in the accompanying paper, CoBLM A2 green binds by partial intercalation 3′ to C6 and inserts through the minor groove.[16,48]

To determine if this mode of binding is unique to this oligomer or to dGpC steps, we have investigated a second self-complementary oligonucleotide d(CCAGTACTGG). This oligomer was chosen as our recent studies revealed that the T of GTAC is a hot spot for ds cleavage by a single molecule of FeBLM, with the ratio of ds:ss cleavage of 1:3.[49] Thus, this oligomer offered an opportunity to examine a GpT step and had the possibility of allowing us to examine how a metallo-BLM might interact with two different cleavage sites without dissociation from the duplex. The preliminary studies are intriguing and informative. First, a major complex of 0.8:1 is formed in slow exchange on the NMR time scale. The bithiazole protons are upfield shifted, indicative of partial intercalation as observed with **1**. Second, a minor complex, 0.2:1, is also readily apparent. This complex has not yet been examined in any detail but could be indicative of the secondary cleavage site of this hot spot for ds cleavage. These studies thus reveal that CoBLM can bind to both GpT and GpC sequences in a similar fashion, giving some hope that the structure reported in detail in the accompanying paper may be a generic one.

Acknowledgment. This research is supported by NIH Grant GM 34454 to J.S. and J.W.K. The NMR facility is supported by NIH Grant P41RR0095. We are grateful to J. Puglisi, J. Battiste, and J. Williamson for many helpful discussions on NMR methods. We are also grateful to S. Woodson for use of her computer equipment.

Supporting Information Available: Expanded NOESY spectrum of CoBLM A2 green and a table comparing proton chemical shifts of different metallo-BLMs (2 pages). This material is contained in many libraries on microfiche, immediately follows this article in the microfilm version of the journal, and can be ordered from the ACS; and can be downloaded from the Internet; see any current masthead page for ordering information and Internet access instructions.

JA9524964

(58) (a) Boger, D. L.; Colletti, S. L.; Honda, T.; Menezes, R. F. *J. Am. Chem. Soc.* **1994**, *116*, 5607−5618. (b) Boger, D. L.; Honda, T.; Dand, Q. *J. Am. Chem. Soc.* **1994**, *116*, 5619−5630. (c) Boger, D. L.; Honda, T.; Menezes, R. F.; Colletti, S. L. *J. Am. Chem. Soc.* **1994**, *116*, 5631−5646. (d) Boger, D. L.; Honda, T. *J. Am. Chem. Soc.* **1994**, *116*, 5647−5656.